Boundary-Layer Meteorol (2011) 138:99–120
DOI 10.1007/s10546-010-9551-7

ARTICLE

Aerodynamic Parameters of Urban Building Arrays with Random Geometries

Sheikh Ahmad Zaki · Aya Hagishima · Jun Tanimoto · Naoki Ikegaya

Received: 4 December 2009 / Accepted: 7 October 2010 / Published online: 26 October 2010

Abstract It is difficult to describe the flow characteristics within and above urban canopies using only geometrical parameters such as plan area index (λ_p) and frontal area index (λ_f) because urban surfaces comprise buildings with random layouts, shapes, and heights. Furthermore, two types of 'randomness' are associated with the geometry of building arrays: the randomness of element heights (vertical) and that of the rotation angles of each block (horizontal). In this study, wind-tunnel experiments were conducted on seven types of urban building arrays with various roughness packing densities to measure the bulk drag coefficient (C_d) and mean wind profile; aerodynamic parameters such as roughness length (z_o) and displacement height (d) were also estimated. The results are compared with previous results from regular arrays having neither 'vertical' nor 'horizontal' randomness. In vertical random arrays, the plot of C_d and z_o versus λ_f exhibited a monotonic increase, and z_o increased by a factor of almost two for $\lambda_f = 48$–70%. C_d was strongly influenced by the standard deviation of the height of blocks (σ) when $\lambda_p \geq 17\%$, whereas C_d was independent of σ when $\lambda_p = 7\%$. In the case of horizontal random arrays, the plot of the estimated C_d against λ_f showed a peak. The effect of both vertical and horizontal randomness of the layout on aerodynamic parameters can be explained by the structure of the vortices around the blocks; the aspect ratio of the block is an appropriate index for the estimation of such features.

Keywords Displacement height · Drag coefficient · Roughness length · Urban building arrays · Wind-tunnel experiments

S. A. Zaki (✉)
Razak School of Engineering and Advanced Technology, University of Technology Malaysia, International Campus, Jalan Semarak, 54100 Kuala Lumpur, Malaysia
e-mail: sheikh_zaki@kyudai.jp

A. Hagishima · J. Tanimoto · N. Ikegaya
Interdisciplinary Graduate School of Engineering Sciences, Kyushu University, 6-1, Kasuga-koen, Kasuga-shi, Fukuoka 816-8580 Japan

1 Introduction

It is important to understand the flow characteristics within and above urban canopies from the viewpoints of the thermal comfort of pedestrians and the dispersion of pollutants. Urban surfaces comprise numerous buildings whose layout, shapes, and heights tend to be irregular or non-uniform, and often extremely random. Hence, it is rather difficult to accurately evaluate wind behaviour above actual urban surfaces using just a few geometrical parameters such as the plan area index (λ_p) and frontal area index (λ_f). In this study, the influence of the 'randomness' of urban geometry on aerodynamic parameters such as drag coefficient C_d, roughness length z_o, and displacement height d has been investigated. In particular, two types of random geometries are examined: a vertical random array and a horizontal random array.

For more than a decade, extensive wind-tunnel experiments, computational simulations, and field observations have been performed in order to understand the aerodynamic features of various urban geometries. Hanna et al. (2002) investigated the mean flow and turbulence within cubical arrays of square and staggered layouts, employing both numerical simulations and hydraulic water flume experiments. They also compared the effect of the layout on the flow of a 'street-canyon'. Stoesser et al. (2003) studied the flow over a cubical array using large-eddy simulations (hereafter LES). Cheng and Castro (2002a) presented the wind characteristics of a staggered cubical array, an aligned cubical array, and a 'random-height' array for $\lambda_p = 25\%$, using a series of wind-tunnel experiments. They reported that the roughness length of a random-height array comprising five blocks of different height is larger than that of a uniform cubical array with the same averaged height. Kanda et al. (2004) systematically investigated the effect of packing densities on turbulent flow characteristics and analysed turbulent organized structures using LES for cubical arrays with $\lambda_p = 3$–44%. Coceal et al. (2006) demonstrated that mean flow structure and turbulence statistics significantly depend on the layout by performing direct numerical simulations (DNS) of the turbulent flow over cubical arrays for staggered, square, and aligned layouts. According to Kanda (2006), the variation in the height of buildings with a square layout has significant effects on both the drag coefficient and turbulent flow structures. Using wind-tunnel experiments, Cheng et al. (2007) analysed the effects of surface geometry on aerodynamic characteristics for uniform cube arrays under two different conditions: $\lambda_p = 25$ and 6.25%. Santiago et al. (2008) performed numerical simulations using a $k-\varepsilon$ turbulence model to quantify the characteristic variations of the sectional drag coefficients of uniform arrays with packing densities $\lambda_p = 6.25$, 11, 16, 25, 33, and 44%. Jiang et al. (2008) performed comprehensive simulations of the airflow over different types of rectangular arrays using LES, and investigated the effect of variations in the building height with a square layout for $\lambda_f = 11\%$. The turbulence characteristics of a uniform array and a random-height array of a staggered layout were compared for $\lambda_p = 25\%$ by Xie et al. (2008) using LES; they used a random-height array that had the same geometry as that employed in the investigation of Cheng and Castro (2002a).

More recently, Hagishima et al. (2009) investigated the effects of variations in the building height using wind-tunnel experiments, and used arrays consisting of only two types of blocks with different heights (hereafter 'two-different-height array') for $\lambda_p = 4.3$, 7.7, 17.4, 30.9, and 39.1%. Kanda and Moriizumi (2009) also observed the bulk transfer coefficient of both momentum and heat using a two-different-height array when $\lambda_p = 25$ and 44%.

In other words, most previous studies investigated arrays with both uniform and non-uniform heights; however, the height variations of actual urban surfaces are not sufficiently reproduced in these works. Meanwhile, some researchers have analyzed the urban morphological characteristics of actual cities using a geographic information system (hereafter GIS).

For example, Burian et al. (2002) reported building height characteristics such as mean value, variance, and histograms using a dataset of the three-dimensional configuration of buildings around downtown Los Angeles, California. Hagishima and Tanimoto (2005) investigated urban configurations using GIS datasets for Tokyo and Fukuoka in Japan and estimated the vertical distribution of the building volume density.

In this study, we first investigate rectangular arrays with variations in height, which we designed based on a statistical analysis using GIS data for Tokyo (Hagishima and Tanimoto 2005), for several values of λ_p.

In contrast to the effect of variations in building height, there have been very few systematic studies on the effects of the random layout of buildings. Hagishima et al. (2009) recently reported results for a square array rotated by 45° and suggested that the effect of wind direction on urban aerodynamic parameters varies significantly with λ_p and λ_f. However, actual urban surfaces consist of streets of various widths and orientations and they also include open spaces; moreover, many buildings are not parallel to the streets. Hence, the geometry of an actual city does not have a regular layout; that is, it is not square or staggered. Therefore, we must also focus on arrays in which the rectangular blocks are rotated randomly. Our study is motivated by the findings of Hagishima et al. (2009), who discussed the effect of layouts and height variations with different packing densities using a series of wind-tunnel experiments. To extend their results, we used similar measurement procedures and investigated both vertical random arrays with different heights as well as horizontal random arrays. Our results for the two types of random arrays are compared with those for regular arrays presented by Hagishima et al. (2009).

In Sect. 2, the theoretical background is given, while Sects. 3 and 4 describe the details of the configuration of arrays and the experimental set-up, respectively. Section 5 describes the evaluation of the representativeness of spatially-averaged wind profiles. The results of the effect of both vertical and horizontal randomness on aerodynamic parameters are discussed in Sects. 6 and 7, respectively, with Sect. 8 presenting the major conclusions.

2 Theoretical Background

We estimated the total surface shear stress of an array by employing direct measurement of the 'form drag' using a floating element. The drag coefficient can be expressed as follows:

$$C_d = \frac{\tau_o}{0.5\rho u_{ref}^2} \tag{1}$$

where τ_o is the total surface shear stress of an urban area, u_{ref} is the reference mean speed, and ρ is the density of air.

The friction velocity u_* is defined as

$$u_* = \sqrt{\frac{\tau_o}{\rho}}, \tag{2}$$

while the vertical profile of the wind speed u_z under neutral conditions can be expressed as follows, using the aerodynamic parameters roughness length z_o and displacement height d,

$$u_z = \frac{u_*}{\kappa} \ln\left(\frac{z-d}{z_o}\right). \tag{3}$$

Here, κ is the von Karman constant, taken equal to 0.4.

The spatially-averaged mean velocity $\overline{u}_z$ for a vertical random array is determined by considering the obstruction of tall blocks as follows:

$$\overline{u}_z = \frac{\sum u_{i,z}}{n}\left(1 - \lambda_{p,z}\right) \tag{4}$$

where $u_{i,z}$ is the wind speed at each point, n is the number of measurement points of the wind speed, and $\lambda_{p,z}$ is the ratio of the area occupied by blocks to the total area at a height z.

We estimated z_o and d by employing the least-squares method using the measurement results of the spatially-averaged mean velocity in the inertial sublayer, and the friction velocity was predetermined by direct measurement of the drag force. The estimation procedure is given in detail in Hagishima et al. (2009).

3 Roughness Arrays

Two types of rectangular arrays were used to investigate the effects of the randomness of urban geometry. The first type focuses on the randomness of the height of the elements, i.e. vertical randomness, while the second consists of blocks that have the same height and shape but are oriented differently, i.e. horizontal randomness. Although actual urban geometry includes various types of randomness, such as variations in both roof shapes and roof areas of buildings, layout pattern, and combinations of the above mentioned factors (e.g. Raupach et al. 2006), our focus here is on the effect of the randomness of the orientation of each block. In order to clarify the dependence of the random orientation of each block, we used arrays consisting of identically shaped blocks. These roughness arrays consist of sharp-edged rectangular blocks made of wood that were glued onto thin plastic plates. Moreover, all the blocks have a uniform base of 25 mm × 25 mm, and hereafter, we assume $L = 25$ mm as the standard length scale.

The schematic diagrams of both the vertical random (hereafter R1.5) and horizontal random arrays (hereafter ST1R and ST1.5R) are shown in Figs. 1 and 2, respectively; features are summarised in Table 1. The numerals 1 and 1.5 refer to the average height of blocks, viz. $1L$ and $1.5L$, respectively.

The R1.5 arrays consisted of nine types of blocks of different height arranged in a staggered layout. The height and fraction of these nine types of blocks are defined using the probability density function (PDF) of the building height derived from Hagishima and Tanimoto (2005). The vertical distribution of the building fraction is found to be as follows:

$$\rho_r\left(z\right) = \rho_r\left(z = 0\right)\exp\left[-\left(\frac{z/H_{ave}}{\phi}\right)^{\gamma}\right], \tag{5}$$

where $\rho_r(z)$ is the ratio of the area occupied by a building to the total area at a height z, H_{ave} is the average height of the buildings, and γ and ϕ are the parameters of the Weibull distribution, which depend on the floor area ratio.

The equation for the PDF of the building height can be expressed by differentiation of Eq. 5 as follows:

$$PDF = \frac{\gamma}{\phi}\left(\frac{z/H_{ave}}{\phi}\right)^{\gamma-1}\exp\left[-\left(\frac{z/H_{ave}}{\phi}\right)^{\gamma}\right]. \tag{6}$$

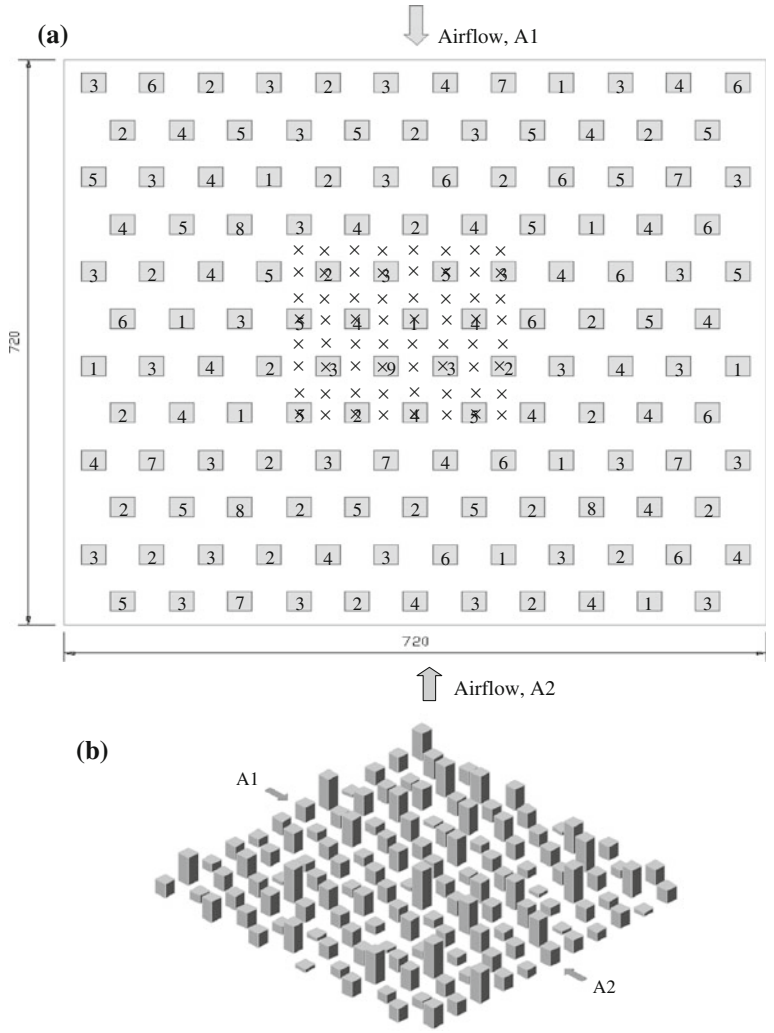

Fig. 1 Staggered vertical random array (R1.5) with $\lambda_p = 17.4\%$. The numeral in each block refers to the block heights (Table 1). *Crosses* indicate the measurement points of the velocity profiles. A1 and A2 refer to the wind direction of the drag measurement (dimensions in mm). **a** Schematic plan view and **b** three-dimensional view

We adopted the parameters $\gamma = 1.39$ and $\phi = 1.08$ based on the results for an area with a floor area ratio from 100 to 160% in Tokyo, as shown in Fig. 3. Next, we simplified the PDF using nine types of blocks of different height, as shown in Fig. 4; the fractions of these blocks were calculated on the basis of the trapezoidal rule with an accuracy of 0.2%.

The allocation of each block in array R1.5 is governed by a somewhat random process. We divided the area covered by the array into eight areas, i.e. A, B, C, D, E, F, G, and H, as shown in Fig. 6, and estimated the quantity of the nine types of blocks for each area based on a PDF. Subsequently, we allocated all the blocks manually so that the configuration of arrays would be random. We used the standard deviation of the height of blocks, σ, to describe the vertical randomness, with σ defined as follows:

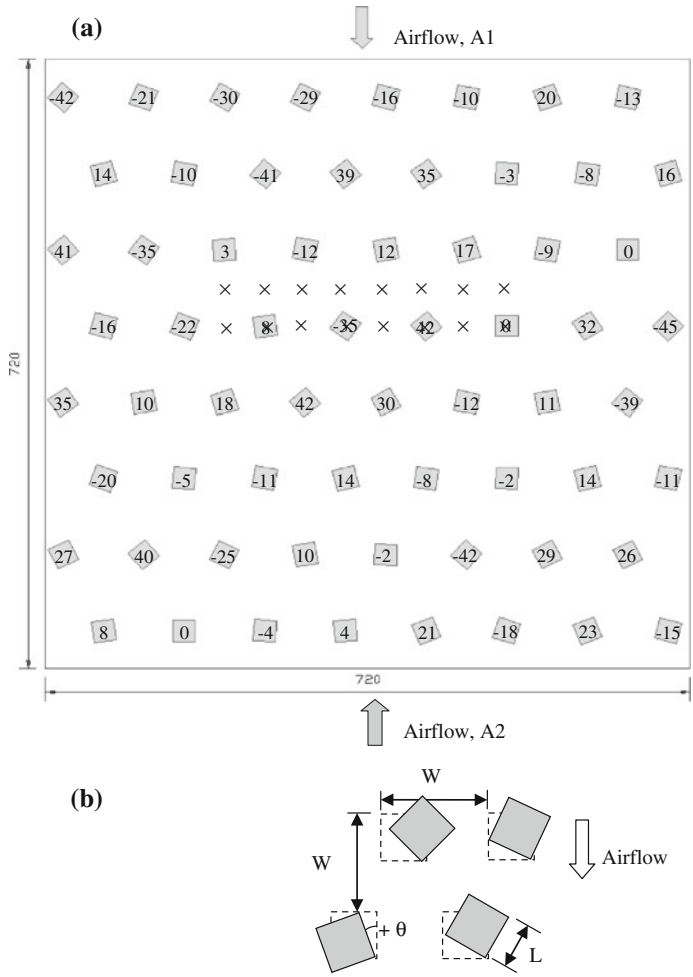

Fig. 2 Distribution of blocks in the horizontal random array (ST1R) for $\lambda_p = 7.7\%$. The number on each block refers to its rotation angle in degrees. *Crosses* indicate the measurement points of velocity profiles. θ refers to the rotation angle of a block, and counter-clockwise is defined as positive (dimensions in mm). **a** Schematic plan view and **b** direction of measurement of the rotation angle

$$\sigma = \sqrt{\frac{1}{n}\sum_{i=1}^{n}(H_i - H_{ave})^2} \tag{7}$$

where n is the total number of blocks in an array, and H_i is the height of each block in an array.

The mean and standard deviation of the block height of the array R1.5 are $1.5L$ and $1.68L$, respectively. The horizontal random array comprises a 'repeating' unit, as shown in Fig. 2, containing 64 blocks that are rotated randomly in a staggered layout. The rotation angle of each block varies within the range of $-45°$ and $+44°$, which is defined based on a random number, the average and standard deviation of each angle are 0° and 23.74°, respectively. We used two arrays with heights of $1L$ and $1.5L$, which we refer to as ST1R and ST1.5R,

Table 1 Roughness arrays

Arrays	Layout	Remarks
R1.5	Staggered	Combination of blocks ($1 = 0.36L$, $2 = 0.84L$, $3 = 1.32L$, $4 = 1.5L$, $5 = 2.0L$, $6 = 2.64L$, $7 = 3.0L$, $8 = 3.32L$, $9 = 3.76L$) $H_{ave} = 1.5L$, $\sigma/H_{ave} = 1.12$
ST1R	Staggered with rotation between $-45°$ to $+44°$	Mean and standard deviation of rotation angle are 0° and 23.74° $H_{ave} = L$
ST1.5R	Staggered with rotation between $-45°$ to $+44°$	Mean and standard deviation of rotation angle are 0° and 23.74° $H_{ave} = 1.5L$

H_{ave} is the average height of blocks, σ is the standard deviation of the height of blocks, and L is the width of all blocks ($L = 25$ mm)

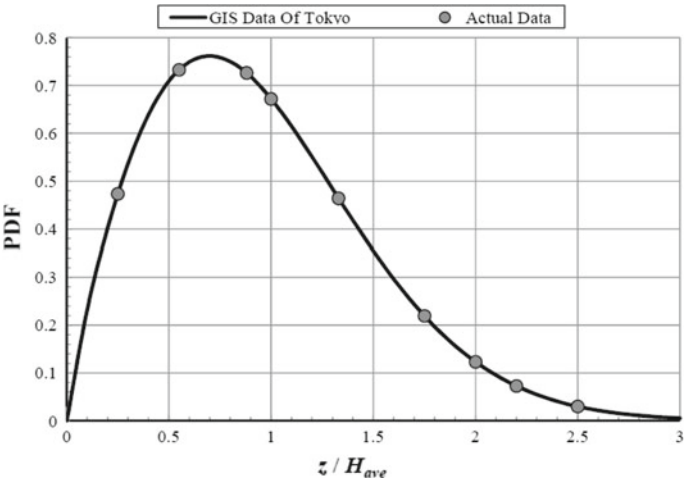

Fig. 3 Probability density function (PDF) of the building height based on a GIS dataset for Tokyo

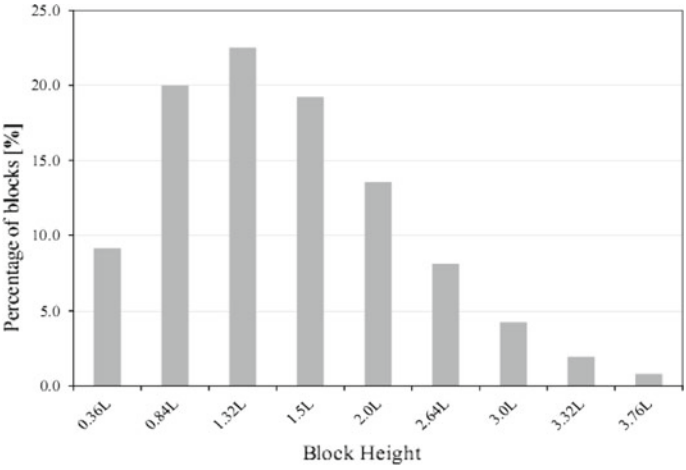

Fig. 4 Histogram of block heights of array R1.5

Table 2 Frontal-area to-roof-area ratio of blocks α_p for staggered uniform arrays, 45° rotated square arrays, and horizontal random arrays

Arrays	Remarks	α_p
ST1	Staggered cubical array ($L \times L \times L$)	1
D1	45° rotated square array ($L \times L \times L$)	1.414
ST1R	Horizontal random array ($L \times L \times L$)	1.244
ST1.5	Staggered uniform array ($L \times L \times 1.5L$)	1.5
D1.5	45° rotated square array ($L \times L \times 1.5L$)	2.121
ST1.5R	Horizontal random array ($L \times L \times 1.5L$)	1.890

respectively. These two types of random arrays are investigated for different packing densities. We used five conditions of λ_p (7.7, 17.4, 30.9, 39.1, and 48.1%) for the R1.5 array, whereas we used three conditions of λ_p (7.7, 17.4, and 30.9%) for the ST1R and ST1.5R arrays. For the ST1R and ST1.5R arrays, λ_f can be defined as

$$\lambda_f = \frac{LH \sum_{i=1}^{n} (\sin\theta_i + \cos\theta_i)}{W^2 n}, \tag{8}$$

where L is the width of the block, H is the height of the block, θ_i is the angle of a block in the counter-clockwise direction, and W is the length of the lot area occupied by a single block.

We adopt an additional geometric parameter, i.e. the frontal-area to roof-area ratio of a roughness element α_p, to explain the morphological characteristics of block rotation, where α_p can be defined as

$$\alpha_p = \frac{A_f}{A_{roof}} = \frac{\lambda_f}{\lambda_p} \tag{9}$$

Here, A_f is the frontal area of the block and A_{roof} is the roof area of the block.

Table 2 lists the values of α_p for the arrays we analysed. The value of α_p becomes larger for the three types of arrays in the following order: a staggered array, a horizontal random array, a square array with 45° rotation. This parameter also indicates the slenderness of each block. The α_p of a block with height $1.5L$ is larger than that of a cube with height $1.0L$ for all types of arrays.

4 Experimental Set-Up

The experiment was performed in a low-speed single-return wind tunnel at the laboratory of the Interdisciplinary Graduate School of Engineering Sciences, Kyushu University, Japan. The working section of this equipment is 1 m high × 1.5 m wide × 8 m long. A schematic side-view and plan-view of the wind tunnel are shown in Figs. 5 and 6, respectively. The surrounding areas that are covered with a roughness array have lengths of 3 and 0.18 m in the windward direction and leeward direction, respectively. The upwind fetch is very significant in boundary-layer development. Cheng and Castro (2002b) investigated the relationship between fetch and the development of the equilibrium layer after a step change in roughness. They indicated that the fetch needed for the equilibrium layer to reach the upper limits of the roughness sublayer was around 300 times the roughness length, using a definition based on a 5% difference in velocity. Hagishima et al. (2009) also studied the effect of fetch on surface shear stress, and reported that the total surface drag of an array decreases rapidly with an

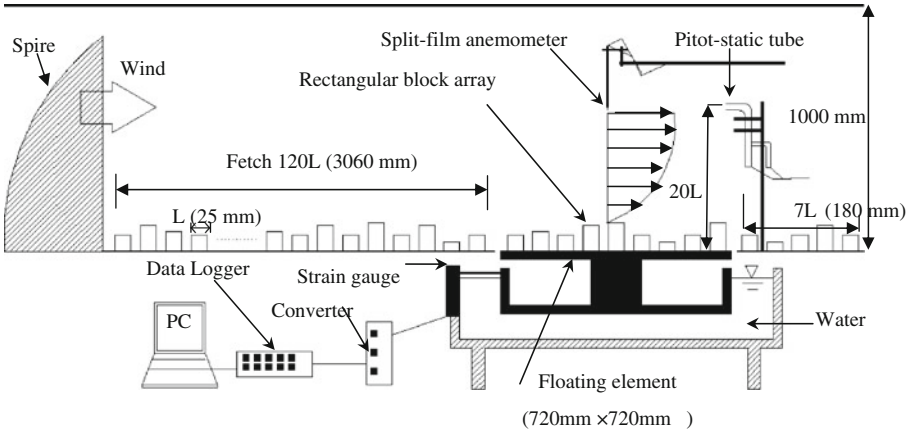

Fig. 5 Side view of wind tunnel set-up

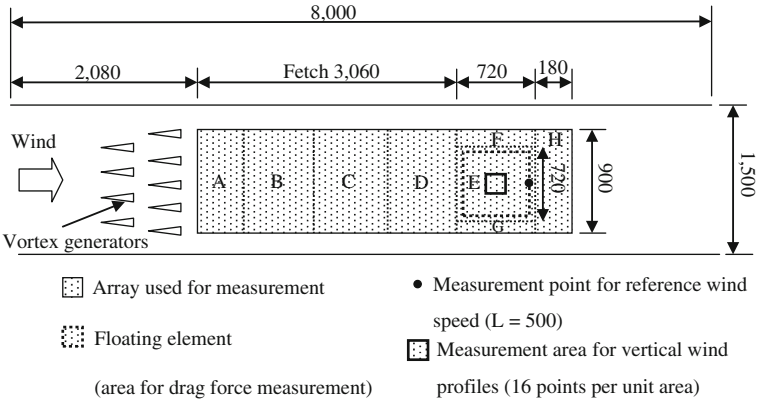

Fig. 6 Schematic plan view of the wind tunnel (dimensions in mm)

increase in fetch from zero to $30L$, and the drag continuously decreases as the fetch increases from $30L$ to $120L$. Although the dependence of the fetch on the total surface drag does not appear to converge, the estimated thicknesses of the boundary layer, inertial sublayer, and roughness length satisfy the requirement for an equilibrium state presented by Cheng and Castro (2002b). We therefore used a fetch of approximately $120L$ ($L = 25$ mm), which is the same as that used in Hagishima et al. (2009).

The total surface drag acting on each array was measured directly using a floating element and a strain gauge (Interface, MB5). The drag force for each array was measured five times and the averaged values were used in our analysis; the variation coefficient of the five measurements was less than 0.2% in all cases. In addition, the spatially-averaged vertical profile of mean wind over the arrays was measured using split-film anemometry. All the measurements described here were conducted under the condition of a free stream velocity of approximately 8 m s^{-1}. The wind-tunnel device and the measurement procedure used in this study are almost identical to those used in Hagishima et al. (2009).

The mean profiles for the vertical random array (R1.5) and horizontal random arrays (ST1R and ST1.5R) were measured at 64 points and 16 points respectively within a horizontal plane,

to obtain a spatially-averaged profile. The mean profiles for the vertical and horizontal arrays are shown in Figs. 1 and 2, respectively. Each vertical profile consists of 28 measurement levels ($0.5L$, $1L$, $1.5L$, $2.0L$, $2.5L$, $3.0L$, $3.5L$, $4.0L$, $4.5L$, $5.0L$, $5.5L$, $6.0L$, $6.5L$, $7.0L$, $7.5L$, $8.0L$, $8.5L$, $9.0L$, $9.5L$, $10.0L$, $10.5L$, $11.0L$, $11.5L$, $12.0L$, $14.0L$, $16.0L$, $18.0L$, and $20.0L$) above the ground. We measured the total drag forces acting on the vertical random array (R1.5) and the horizontal random arrays (ST1R and ST1.5R) with two different wind directions (A1 and A2), as shown in Figs. 1 and 2, under all conditions of packing density, because the array is random in terms of the allocation of roughness elements. The measured values of the drag force with the two wind directions are in good agreement, and the discrepancy is less than 0.5% for all arrays. This result implies that the arrays are fairly uniform and random. Therefore, we use the average of the two conditions of wind direction as the representative value in the following discussion.

The results for R1.5 are compared with those for a uniform array (hereafter ST1.5) and two-different-height arrays (ST1.5-st and ST1.5-sq), which were investigated by Hagishima et al. (2009). In contrast, the results for ST1R and ST1.5R were compared with those for a cubical staggered array (hereafter ST1), a cubical 45° rotated array (hereafter D1), a uniform staggered array with a height of 1.5L (ST1.5), and a uniform 45° rotated array with a height of 1.5L (hereafter D1.5), which were investigated by Hagishima et al. (2009). The α_p values for the horizontal random arrays, staggered uniform arrays, and 45° rotated square arrays are listed in Table 2. From these comparisons, we make detailed estimates of the effects of randomness on the drag force and aerodynamic parameters.

In our study, the Reynolds number (Re) is based on the free stream velocity at $20L$ and the average height, and ranges from approximately 1.3×10^5 to 2.0×10^5; the roughness Reynolds number (Re_*) is based on friction velocity and the roughness length and ranges from approximately 121 to 164. Thus, a fully rough turbulent flow appears to exist, and the dependence of Re on aerodynamic parameters is probably negligible, as was also determined by Perry et al. (1969) and Snyder and Castro (2002).

5 Evaluation of the Representativeness of Spatially-Averaged Wind Profiles

Di Sabatino et al. (2008) reported that the determination of the spatially-averaged velocity depends on the height variability of buildings and the morphometry of the immediate area. In our experiment, the arrangements of the two types of random arrays were designed based on statistical fluctuations, and an array located on the floating element used for the drag-force measurement did not comprise a repeating unit. Therefore, to obtain a spatially-averaged profile with sufficient representativeness for an array, it is desirable to obtain wind profiles at numerous points. We measured mean wind profiles at 64 points and 16 points for the vertical and horizontal random arrays, respectively, as mentioned earlier, and calculated spatially-averaged mean profiles using these measurements. In order to confirm the validity of the spatial representativeness of the estimated profiles, we investigated the data as follows.

First, we calculated the averaged mean wind profiles based on 16-point measurements and 64-point measurements for a vertical random array, and confirmed that the difference between the spatially-averaged mean profiles normalized by the mean value at $20L$ is less than 0.8% for each height. In the case of horizontal random arrays, we compared the profiles similarly, based on 12-point measurements and 16-point measurements. The discrepancy between the two is less than 0.5% for each height. Second, we compared the deviation of the wind speed of the vertical random array and horizontal random arrays at $2.0L$ and $1.5L$, respectively, using a different number of measurement points. Figure 7 presents a histogram

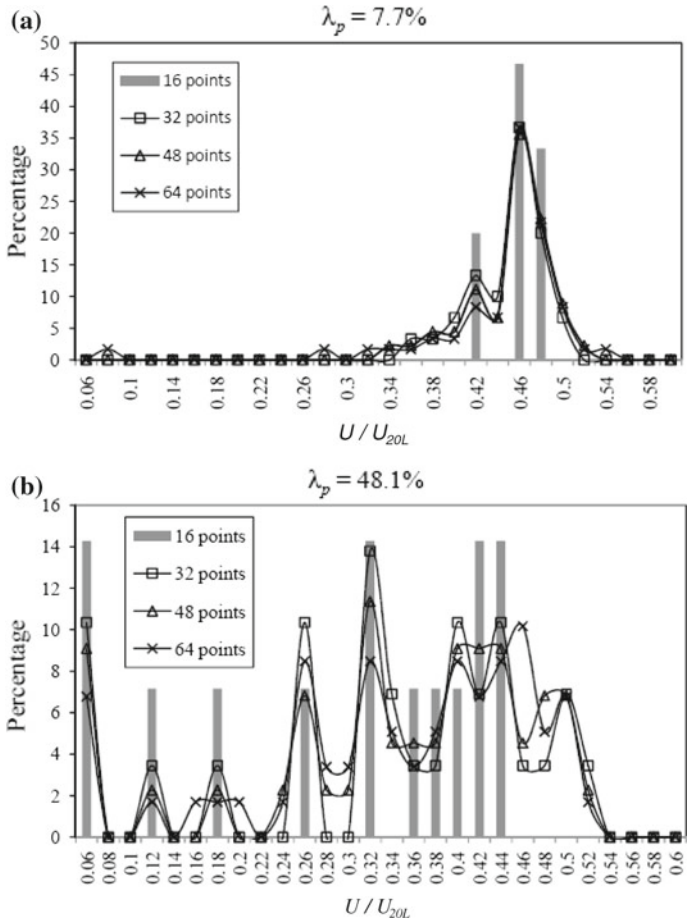

Fig. 7 Histogram of normalised mean velocity of the vertical random array at $z = 2L$ based on the values of 16, 32, 48, and 64 measurement points. **a** $\lambda_p = 7.7\%$ and **b** $\lambda_p = 48.1\%$

of the normalised mean velocity of array R1.5 at $z = 2.0L$ based on the values of different numbers of measurement points for $\lambda_p = 7.7\%$ and $\lambda_p = 48.1\%$. As can be seen in the figure, the normalised wind speed of 16-point measurements for $\lambda_p = 7.7\%$ is in the range of 0.42–0.48. In contrast, the distribution of 32-point measurements is scattered in a wide range; the deviation pattern gradually converges for 48-point to the 64-point measurements. In the case of high λ_p, we can clearly recognise a similar tendency in spite of the larger deviation. Since the number of blocks arranged on a floating area depends on λ_p, the ratio of the measured area for wind speed to the total area of a floating element differs depending on the value of λ_p. For example, the 64-point measurements for $\lambda_p = 7.7$, 17.4, 30.9, 39.1, and 48.1% cover 25, 11.6, 6.3, 5, and 4% of the area of the total floating element, respectively. In spite of this, the tendency shown in Fig. 7 implies that the profiles based on 64-point measurements are spatially representative of a vertical random array.

For the horizontal random arrays (ST1R and ST1.5R), a comparison of the distribution of normalised mean velocity at $z = 1.5L$ for 8, 12, and 16 point-measurements for $\lambda_p = 7.7$ and 30.9% are shown in Figs. 8 and 9. The deviation pattern gradually converges from the

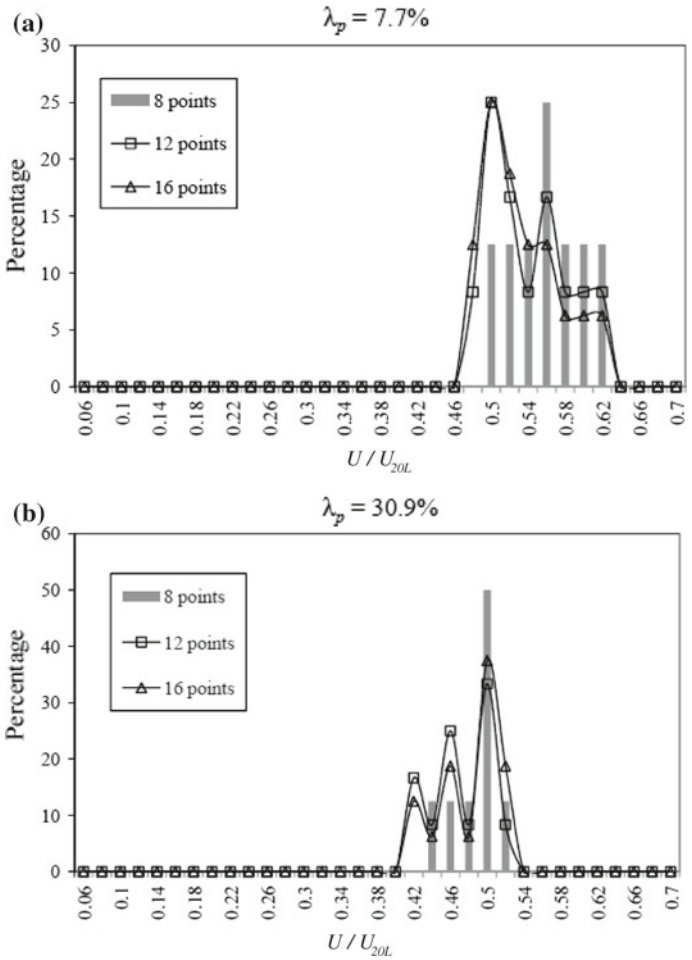

Fig. 8 Comparison of distribution of normalised mean velocity of the horizontal random array with average height $1L$ at $z = 1.5L$ for 8-, 12-, and 16-point measurements. **a** $\lambda_p = 7.7\%$ and **b** $\lambda_p = 30.9\%$

12- to 16-point measurements, and it might be concluded that 16-point measurements for a horizontal random array produce a fairly good representation of a spatially-averaged profile.

Although we present a portion of all the comparison results herein, all the residual graphs display a tendency similar to that shown in Figs. 7, 8, and 9. We therefore concluded that the estimated averaged profiles reflect well the characteristics of the random arrays.

6 Results of Vertical Random Arrays

6.1 Drag Coefficient C_d

The relationships between the estimated C_d of a vertical random array (R1.5) and various values of λ_p are shown in Fig.10; the reference mean speed is defined at a height of $20L$.

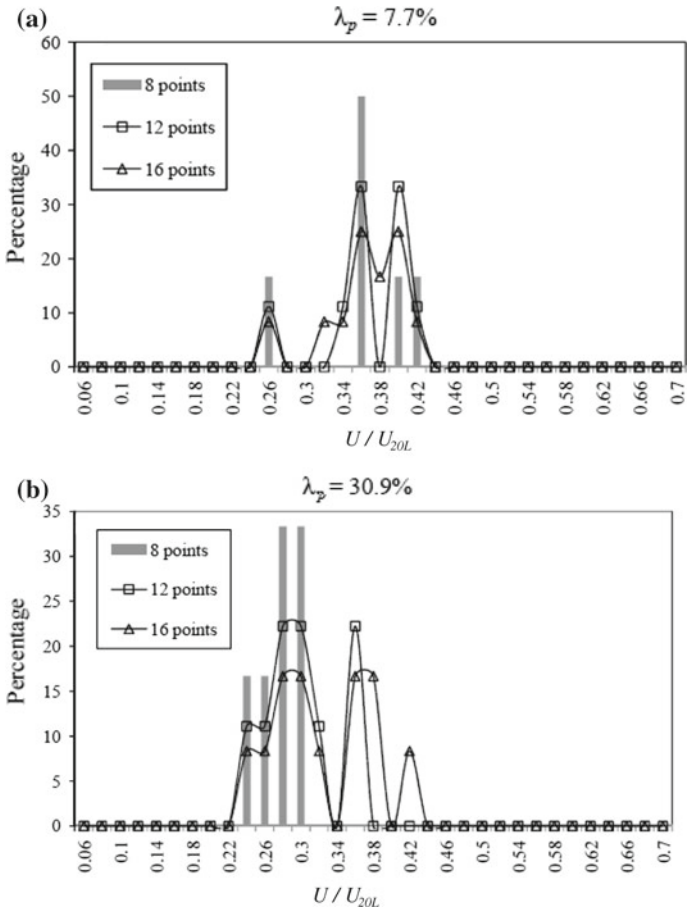

Fig. 9 Comparison of distribution of normalised mean velocity of the horizontal random array with average height $1.5L$ at $z = 1.5L$ for 8-, 12-, and 16-point measurements. **a** $\lambda_p = 7.7\%$ and **b** $\lambda_p = 30.9\%$

The results for the two-different-height arrays (ST1.5-st and ST1.5-sq) and uniform height array (ST1.5) presented by Hagishima et al. (2009) are also plotted as a reference. As can be seen from the data given in Fig. 10, the C_d of the uniform staggered array ST1.5 has a small maximum at $\lambda_p = 7.7\%$. However, for ST1.5-st and ST1.5-sq, the estimated C_d increased almost monotonically with λ_p and was larger than that of the array of ST1.5 when λ_p exceeded 32%. In the case of R1.5, C_d increases slightly from $\lambda_p = 7$–32% and increases dramatically when λ_p exceeds 32%. This monotonic increase in the C_d of R1.5 suggests a hypothesis. The hypothesis is that the C_d of an array with a highly vertical randomness increases monotonically with λ_p not only when $\lambda_p \leq 48\%$, but also when $\lambda_p \geq 48\%$. As can be observed in Figs. 3 and 4, R1.5 has large deviations in block height from $0.36L$ to $3.76L$, and the height histogram leans to the left (short block). In this regard, Xie et al. (2008) pointed out that tall buildings have a significant effect on the total drag of a building array with non-uniform heights. This implies that the peak of the C_d–λ_p curve of an array with height variations is dominated by the condition of whether the flows around tall blocks interfere with each other. It would be difficult for the flows around the

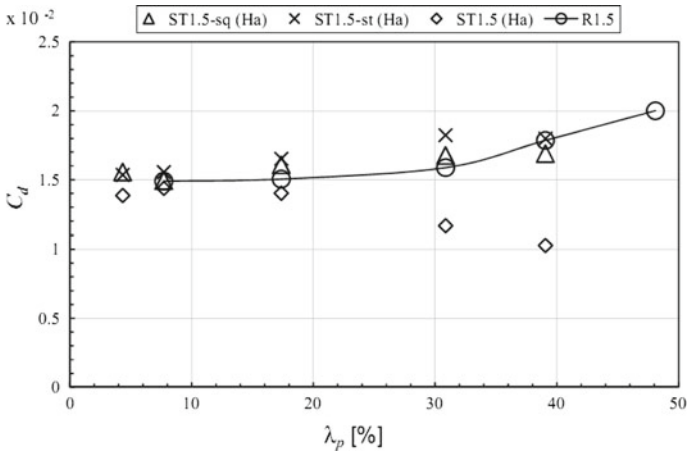

Fig. 10 Drag coefficient C_d for arrays with vertical randomness under various λ_p conditions. For comparison, the results for the two-different-height arrays and uniform arrays are shown. The characterisation of the R1.5 array refers to Table 1

sparsely scattered tall blocks of R1.5 to have mutual interference due to the large distance between them. Therefore, the well-known 'skimming flow regime' might not take place under any λ_p condition. This implies that the skimming flow regime is not present in an urban area with a high heterogeneity of building heights, in spite of the building coverage ratio, except for a region in which particularly tall buildings are concentrated in a central core.

Next, we discuss the relationship between the standard deviation of the height of blocks, σ, and the drag coefficient C_d. Figure 11 shows C_d for the two-different-height arrays (ST1.5-sq) and a vertical random array (R1.5), which was scaled by the value for the uniform array (ST1.5) under the same conditions of λ_p and average height. The results based on the outdoor scale model experiment of Kanda and Moriizumi (2009) are also displayed for comparison. The C_d values are almost independent of the standard deviation of heights when $\lambda_p = 7.7\%$. In contrast, C_d increases and decreases with σ/H_{ave} when $\lambda_p = 17.4$ and 30.9%, respectively. On the other hand, C_d increases monotonically as σ/H_{ave} increases when $\lambda_p = 39.1\%$, indicating that C_d is significantly affected by the standard deviation of the height of blocks when $\lambda_p \geq 17\%$. This tendency is similar to that noted in Kanda and Moriizumi (2009).

6.2 Roughness Length z_o and Displacement Height d

The estimated z_o and d of vertical random arrays scaled by an averaged block height H_{ave} are shown in Fig. 12, and those for ST1.5-st, ST1.5-sq, and ST1.5, as well as a prediction based on Macdonald et al. (1998) are also shown for comparison. The z_o/H_{ave} tendency for the vertical random array (R1.5) is considerably different from that for a uniform staggered array (ST1.5) and the two-different-height arrays (ST1.5-st and ST1.5-sq).

The z_o/H_{ave}–λ_f curves for the three arrays (ST1.5, ST1.5-st, and ST1.5-sq) have gentle peaks, a tendency that is identical to that noted in previous studies on the flow regime of uniform arrays (e.g. Grimmond and Oke 1999). In contrast, the estimated z_o/H_{ave} of the array R1.5 increases slightly for $\lambda_f = 11$–48% and significantly increases when $\lambda_f \geq 48\%$;

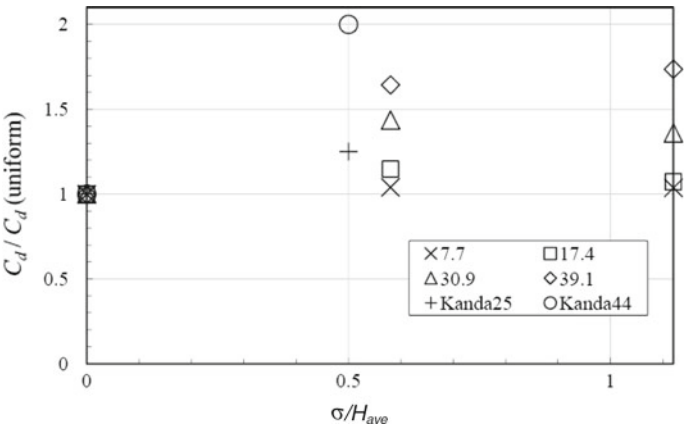

Fig. 11 Effects of the standard deviation of the height of blocks on the drag coefficient ratio for the two-different-heights array (ST1.5-sq), vertical random array (R1.5), and uniform array (ST1.5) for various λ_p values. The *Crosses* (Kanda25) and *unfilled circle* (Kanda44) denote the drag measurements when $\lambda_p = 25$ and 44%, respectively, which were obtained in outdoor scale model experiments of Kanda and Moriizumi (2009). The values for Kanda and Moriizumi (2009) are scaled on the shear stress of a uniform array

this is similar to the tendency for C_d. This result may reflect the fact that the vortices generated around sparsely arranged tall blocks that generate a relatively large portion of the total drag tend to display less of a tendency toward interference; moreover, it is hard for a typical skimming flow to be generated over an array characterized by highly vertical randomness (as mentioned previously). Coceal et al. (2006) investigated the mean flow structure of cubical squares and staggered arrays using DNS, and noted that the development of a counter-rotating vortex depends significantly on the distance between two cubical blocks. In fact, the gap between two blocks is considerably closer in a square layout than in a staggered array, and thus, the flow recirculation that appears between two blocks of a square layout is stronger.

The d/H_{ave} values for the arrays with vertical randomness also display tendencies that are completely different from those in previous studies on uniform arrays (e.g. Macdonald et al. 1998), in that the monotone convex increases from 0 to 1. Our results indicate that the effect of height variability on d varies with λ_p. For example, d/H_{ave} for R1.5 increased from $\lambda_p = 17\%$ to $\lambda_p = 31\%$, while it decreased sharply to 0.6 when $\lambda_p = 48\%$. At the same time, the estimated d/H_{ave} values for the two-different-height arrays are five times larger than for a uniform staggered array under the condition of $\lambda_p = 7\%$. In contrast, d/H_{ave} for R1.5 for $\lambda_p = 7\%$ is eight times larger than it is for ST1.5 and twice as large as it is for the two-different-height arrays. On the other hand, the discrepancy between d/H_{ave} for a vertical random array and the two-different-height arrays is extremely small when λ_p is more than 17%. Apparently, the effect of tall blocks on displacement height is more pronounced under the condition of sparse packing density.

Another interpretation can be obtained by comparisons with previous work, as shown in Fig. 13. The results of Jiang et al. (2008) for non-uniform arrays with a square layout as estimated using LES for $\lambda_f = 11\%$ is plotted as a reference. All the values for d/H_{ave} estimated by the present work and by Hagishima et al. (2009) have a consistent linear correlation with the standard deviation of height (σ/H_{ave}) when $\lambda_p \leq 30.9\%$, even though there are only three plots for each λ_p condition. This tendency is similar to that shown in the data of

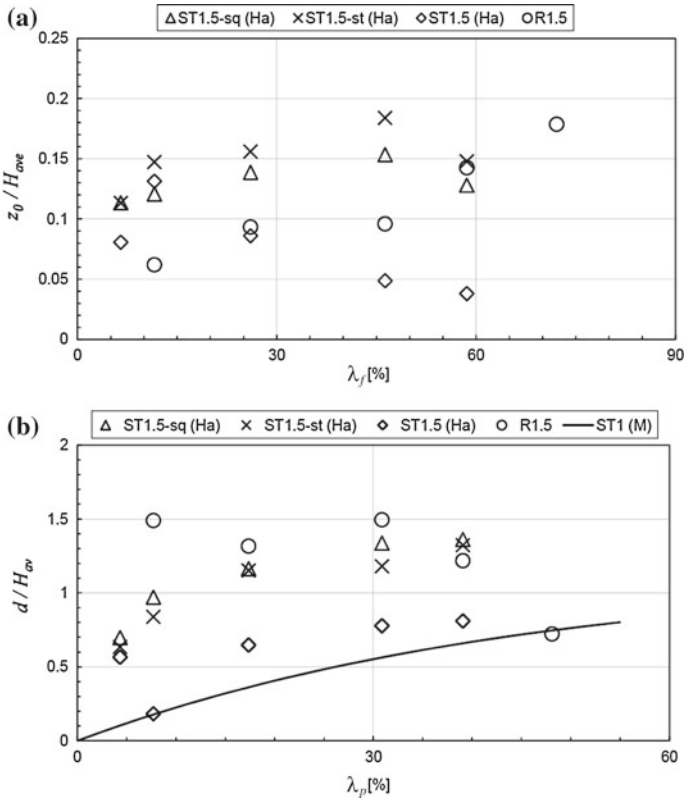

Fig. 12 Estimated aerodynamic parameters for arrays with vertical randomness. For comparison, the results for the two-different-heights arrays and uniform arrays are shown. The characterisation of the R1.5 array refers to Table 1. ST1.5-sq (Ha), ST1.5-st (Ha), and ST1.5 (Ha) refer to the estimations of Hagishima et al. (2009). ST1 (M) refers to values for the staggered cubical array estimated on the basis of the model proposed by Macdonald et al. (1998)

Jiang et al. (2008); hence, such a tendency of d to increase against (σ/H_{ave}) might be considered conclusive. On the other hand, the d/H_{ave} values when $\lambda_p = 39.1\%$ fluctuate from zero to 1.1 over the range of σ/H_{ave} making it probable that the dependence of σ/H_{ave} on d/H_{ave} varies with the condition of λ_p.

7 Results of Horizontal Random Arrays

7.1 Drag Coefficient C_d

The estimated C_d values for horizontal random arrays (ST1R and ST1.5R) under various values of λ_f are shown in Fig. 14; the reference mean speed is defined at a height of $20L$, and those for uniform staggered arrays (ST1, ST1.5) and 45° rotated square arrays (D1, D1.5) presented by Hagishima et al. (2009) are also plotted as a reference.

The $C_d - \lambda_f$ plots for all the arrays show mild peaks, with the exception of the ST1.5R array. This tendency of ST1.5R may be attributed to the fact that only three λ_f values were

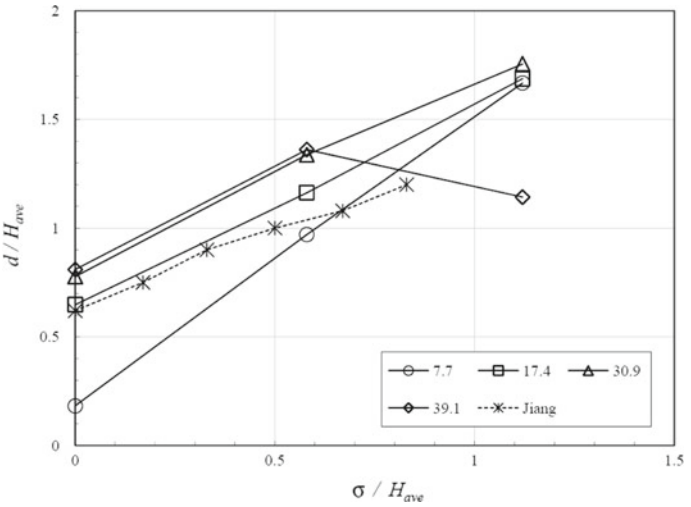

Fig. 13 Effects of standard deviation of the height of a block on displacement height for various λ_p values. *Cross* (Jiang) denotes the LES method for $\lambda_f = 11\%$

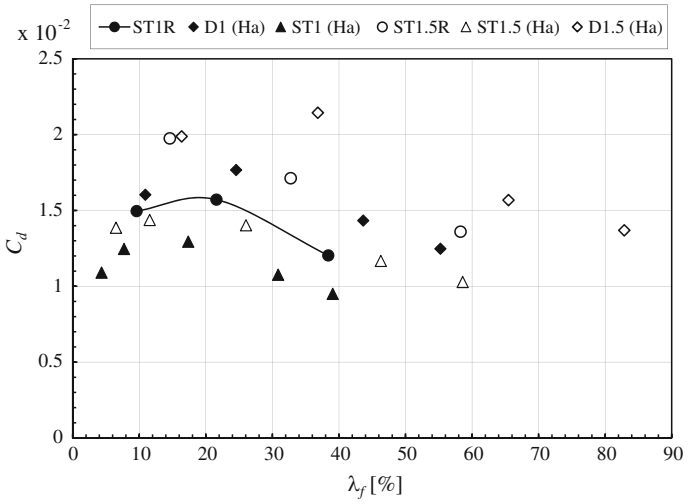

Fig. 14 Drag coefficient C_d for arrays with horizontal randomness under various λ_f conditions. As a reference, the results for a cubical staggered array (ST1), cubical 45° rotated array (D1), ST1.5, and uniform 45° rotated array (D1.5) are shown. The characterisation of the ST1R and ST1.5R arrays refer to Table 1, but for D1, ST1, ST1.5, and D1.5 refer to Hagishima et al. (2009)

used in the measurements; moreover, it is probable that the C_d peak for ST1.5R would be located between ST1.5 and D1.5 if we measured C_d for different λ_f values. In addition, the peak value of C_d increases in the arrays in the following order: staggered arrays, horizontal random arrays, and 45° rotated arrays; the λ_f condition for which C_d has a maximum value also increases in the same order. In other words, among the three arrays, it is extremely difficult for the airflow over a 45° rotated square array to undergo transition from the wake interference flow to skimming flow under identical λ_f conditions, whereas it is easier for the

airflow over a staggered array. This tendency indicates that λ_f cannot universally explain the aerodynamic effect of the rotation angle of the blocks, even though λ_f takes into account the increase in the frontal projecting area that is due to block rotation, as shown in Fig. 2b and Eq. 8.

The λ_f condition for a flow regime transition differs among the three types of arrays due to the characteristics of flow around a cube with different rotation angles. If the wind is perpendicular to the upstream face of a cube, counter-rotating vortices will clearly develop at the lower layer of the front of the block. In contrast, if a cube is rotated 45° to the mean wind direction, no counter-rotating vortices appear in front of the lateral edges of the cube, as reported by Hansen and Cermak (1975) and Plate (1982). Since a reverse flow and counter vortex within a canopy is typical of the mean flow of the skimming regime for a regular block array, the ease with which counter vortices are generated around a block is related to the transience of the flow regime over an array consisting of such blocks. Therefore, an array of blocks that are rotated 45° tends to hinder the generation of counter vortices, and thus, the skimming regime does not form as easily as it does in the case of a staggered array under the same λ_f conditions. In a similar manner, we can predict that a horizontal random array is more streamlined than a staggered array and less streamlined than a 45° rotated array. Hence, the λ_f value of the C_d peak is higher than it is for a staggered array and lower than it is for a 45° rotated array.

Next, Fig. 15 explains the relationship between the maximum value of drag coefficient C_d for each type of array and the frontal-area to roof-area ratio of the block α_p. It indicates that the momentum absorption produced by a regular block array with a roughness density condition in which the roughness functions most effectively, has an approximately linear relation to the parameter α_p. A horizontal random array ST1R with $\alpha_p = 1.244$ shows a larger maximum C_d as compared with ST1 with $\alpha_p = 1$, and a smaller maximum value compared with D1 with $\alpha_p = 1.414$. A similar tendency can be observed for the arrays with an average height of $1.5L$. In other words, the parameter α_p indicates the ease of flow transition for each layout pattern. For example, it is difficult for an array with a higher α_p to undergo transition from the present type of flow into a skimming flow and it can be categorized as a less bluff-body type roughness.

7.2 Roughness Length z_o and Displacement Height d

The determined aerodynamic parameters scaled by the averaged height of arrays are displayed in Fig. 16; the curves for the uniform staggered arrays (ST1, ST1.5) and 45° rotated square arrays (D1, D1.5) presented by Hagishima et al. (2009) are also plotted as a reference. In addition, the results for a staggered cubical array that are estimated based on the model proposed by Macdonald et al. (1998) and for a cubical square array based on logarithmic fitting using the results of LES by Kanda et al. (2004) are plotted as a reference.

The curves of z_o/H_{ave} against λ_f for ST1, ST1.5, and ST1R show sharp peaks, a tendency that is consistent with previous studies of staggered cubical arrays presented by Macdonald et al. (1998). In contrast, we do not observe similar peaks for D1, D1.5, and ST1.5R due to there being only three plots for each array. The simultaneously estimated d values for ST1.5R at $\lambda_p = 7.7\%$, D1 at $\lambda_p = 7.7\%$, and D1.5 at $\lambda_p = 17.4\%$ were equal to the height of the blocks, which is the condition of constraint used in the non-linear least-squares method. Considering the physical meaning of the parameter d (e.g. Jackson 1981), they should be less than the block height; hence, the unreasonable estimation values are not included in Fig. 16. If we add the parameters based on additional experiments for several different λ_f conditions

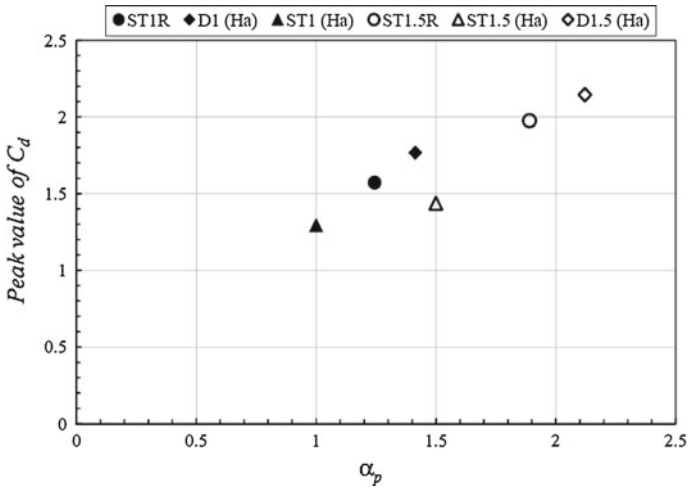

Fig. 15 Effect of frontal-area to-roof-area ratio of blocks, α_p, on drag coefficient for horizontal random arrays (ST1R and ST1.5R), uniform arrays (ST1 and ST1.5), and a cubical 45° rotated array

with numerous measurement points for the wind speed, the tendency of z_o for all arrays may show the above mentioned peaks.

Despite these limitations, we can compare the tendency of z_o for the three types of arrays. The z_o/H_{ave} for ST1.5R and D1.5 are considerably larger than that for ST1.5 when $\lambda_f \geq 15$. Hagishima et al. (2009) reported that the wind direction is the main factor that can produce an increase in the roughness length of square arrays. The difference in z_o among the three types of arrays when λ_f is high can be explained in the same manner as the difference for C_d. The horizontal random array generates weaker counter-rotating vortices than a staggered array, and may form a less streamlined flow field with a 45° rotated square array.

The tendency of the curve of d/H_{ave} versus λ_p for the horizontal random arrays (ST1R and ST1.5R) exhibits an increase in convexity, which is consistent with well-known previous studies (e.g. Macdonald et al. 1998; Kanda et al. 2004). There is a considerable discrepancy between ST1 and ST1.5 when $\lambda_p = 17.4$ and 30.9%, a discrepancy that is similar to the case of the 45° rotated square arrays (D1 and D1.5) when $\lambda_p = 30.9\%$. However, the discrepancy between d/H_{ave} for ST1R and for ST1.5R is small. This indicates that the aspect ratio of the blocks does not affect the vertical distribution of shear stress within a horizontal random array under the condition of high packing densities.

8 Conclusions

We performed a series of wind-tunnel experiments using seven types of urban building arrays with both vertical and horizontal randomness with various packing densities, and we estimated the parameters C_d, z_o, and d. In addition, we compared the obtained results with previous studies of several regular block arrays.

In the case of a vertical random array with variations in block height, the geometry was designed to be representative of the city of Tokyo. This type of array showed a monotonic increase in C_d with an increase in λ_p across a wide range of λ_p from 7 to 48%. This was probably caused by the fact that the flows around the tall blocks of a highly random

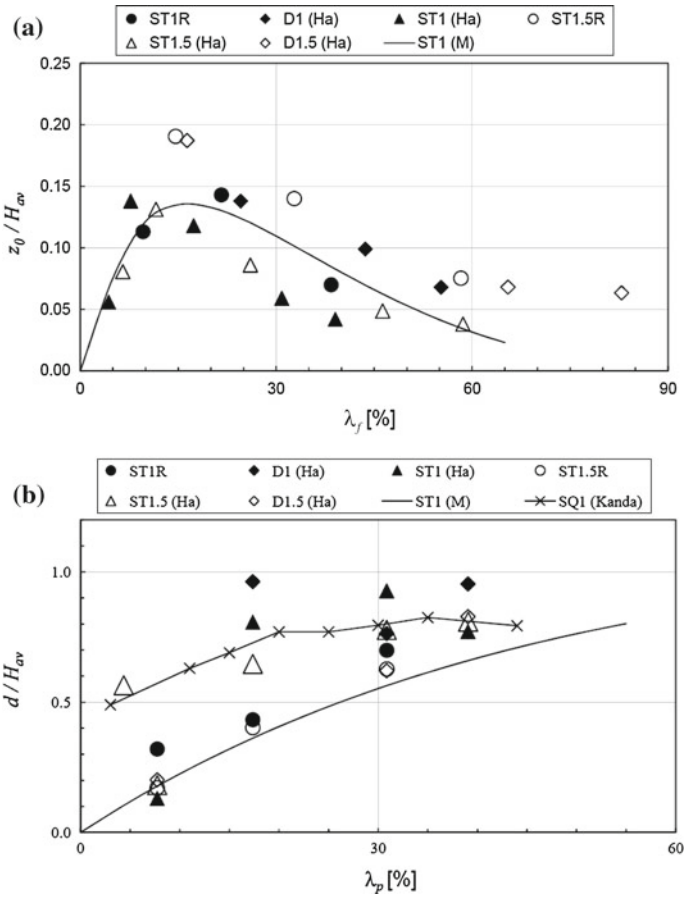

Fig. 16 Estimated aerodynamic parameters for horizontal random arrays. For comparison, the results for staggered arrays (ST1 and ST1.5) and 45° rotated array (D1 and D1.5) (Hagishima et al. 2009) are shown. ST1 (M) refers to values for the staggered cubical array that are estimated based on the model proposed by Macdonald et al. (1998). SQ1 (Kanda) refers to the estimations of Kanda et al. (2004) for cubical square arrays based on logarithmic fitting using the results of LES. The characterisation of the ST1R and ST1.5R arrays refer to Table 1. **a** Roughness length versus λ_f, and **b** displacement height d versus λ_p

vertical array do not interfere with one another due to the large gap between them. Hence, it is difficult for the skimming flow regime to be generated above an actual urban area that has high vertical randomness under any λ_p condition. The effect of the standard deviation of the block height on C_d was particularly remarkable when $\lambda_p \geq 17\%$. The z_o/H_{ave} versus λ_f curve for this array had a similar tendency with C_d, and the increase in z_o/H_{ave} for $\lambda_f = 48$–70% approaches a factor of almost two. The estimated values of d/H_{ave} for the vertical random arrays are completely different from the convex increasing curve reported by Macdonald et al. (1998) that satisfies the two constraints of $d/H_{ave} = 0$ at $\lambda_p = 0$ and $d/H_{ave} = 1$ at $\lambda_p = 100\%$. In particular, the discrepancy between the d/H_{ave} of Macdonald's curve and the present data with a standard deviation of the block heights of $1.68L$ and $0.58L$ was remarkable under the sparse condition of $\lambda_p = 7\%$. This suggests that it is necessary to improve the modelling of z_o and d for arrays with a variation in height.

In the case of horizontal random arrays, the estimated C_d showed a peak when plotted against λ_f, and both the peak values of C_d and the λ_f condition for the peak C_d value increased in the following order: staggered arrays, horizontal random arrays, and 45° rotated square arrays. We attribute this behaviour to the characteristics of flow around single cubes with different rotation angles. A horizontal random array may be more streamlined than a staggered array and bluffer than a 45° rotated square array. Such a tendency might universally be explained by the frontal-area to roof-area ratio α_p, which reflects the aerodynamic effect that is due to both the slenderness and rotation angle of a block. The estimated z_o/H for horizontal random arrays and 45° rotated arrays with a block height of $1.5L$ are considerably larger than those for a uniform staggered array under the condition of $\lambda_f > 15\%$. The effect of block heights of $1L$ and $1.5L$ on the displacement height of horizontal random arrays was less remarkable than that for the uniform staggered arrays and 45° rotated arrays, especially for $\lambda_p > 17\%$. Therefore, considering the statement of Jackson (1981), differences in block height have a small influence on the vertical distribution of the drag force acting on a horizontal random array with high packing densities.

Finally, we point out that the effect of random geometry on aerodynamic parameters is significant for understanding the airflow around buildings in an actual urban city. Such information will be vital to the improvement of numerical models for the prediction of urban climate and dispersion factors.

Acknowledgements This research was financially supported by a Grant-in Aid for Scientific Research (19360260) from the Ministry of Education, Science and Culture of Japan.

References

Burian SJ, Brown MJ, Linger SP (2002) Morphological analyses using 3D building databases, Los Angeles, California. LA-UR-02-0781, Los Alamos National Laboratory, Los Alamos, 66 pp

Cheng H, Castro IP (2002a) Near wall flow over urban-like roughness. Boundary-Layer Meteorol 104: 229–259

Cheng H, Castro IP (2002b) Near-wall flow development after a step change in surface roughness. Boundary-Layer Meteorol 105:411–432

Cheng H, Hayden P, Robins AG, Castro IP (2007) Flow over cube arrays of different packing densities. Boundary-Layer Meteorol 95:715–740

Coceal O, Thomas TG, Castro IP, Belcher SE (2006) Mean flow and turbulence statistics over groups of urban-like cubical obstacles. Boundary-Layer Meteorol 121:491–519

Di Sabatino S, Solazzo E, Paradisi P, Britter R (2008) A simple model for spatially-averaged wind profiles within and above an urban canopy. Boundary-Layer Meteorol 127:131–151

Grimmond CSB, OKE TR (1999) Aerodynamic properties of urban areas derived from analysis of surface form. J Appl Meteorol 38:1262–1292

Hagishima A, Tanimoto J (2005) Investigations of urban surface conditions for urban canopy model. Build Environ 40:1638–1650

Hagishima A, Tanimoto J, Nagayama K, Meno S (2009) Aerodynamic parameters of regular arrays of rectangular blocks with various geometries. Boundary-Layer Meteorol 132:315–337

Hanna SR, Tehraniana S, Carissimoa B, Macdonald RW, Lohner R (2002) Comparisons of model simulations with observations of mean flow and turbulence within simple obstacle arrays. Atmos Environ 33:5067–5079

Hansen AC, Cermak JE (1975) Vortex-containing wakes of surface obstacles. Project THEMIS Technical Report No. 29, Civil Engineering, Department Colorado State University ADA019785, 163 pp

Jackson PS (1981) On the displacement height in the logarithmic velocity profile. J Fluid Mech 111:15–25

Jiang D, Jiang W, Liu H, Sun J (2008) Systematic influence of different building spacing, height and layout on mean wind and turbulent characteristics within and over urban building arrays. Wind Struct 11:275–289

Kanda M (2006) Large-eddy simulations on the effects of surface geometry of building arrays on turbulent organized structures. Boundary-Layer Meteorol 118:151–168

Kanda M, Moriizumi T (2009) Momentum and heat transfer over urban-likes surfaces. Boundary-Layer Meteorol 131:385–401

Kanda M, Moriwaki R, Kasamatsu F (2004) Large eddy simulation of turbulent organized structure within and above explicitly resolved cube arrays. Boundary-Layer Meteorol 112:343–368

Macdonald RW, Griffiths RF, Hall DJ (1998) An improved method for estimation of surface roughness of obstacle arrays. Atmos Environ 32:1857–1864

Perry AE, Schofield WH, Joubert PN (1969) Rough wall turbulent boundary layers. J Fluid Mech 37:383–413

Plate EJ (ed) (1982) Engineering meteorology: studies in wind engineering and industrial aerodynamics, vol 1. Elsevier, Amsterdam, 740 pp

Raupach MR, Hughes DE, Cleugh HA (2006) Momentum absorption in rough-wall boundary layers with sparse roughness elements in random and clustered distributions. Boundary-Layer Meteorol 120: 201–218

Santiago JL, Coceal O, Martilli A, Belcher SE (2008) Variation of the sectional drag coefficient of a group of buildings with packing density. Boundary-Layer Meteorol 128:445–457

Snyder WH, Castro IP (2002) The critical Reynolds number for rough-wall boundary layers. J Wind Eng Ind Aerodyn 90:41–54

Stoesser T, Mathey F, Frohlich J, Rodi W (2003) LES of flow over multiple cubes. Ercoftac Bull 56:15–19

Xie Z-T, Coceal O, Castro IP (2008) Large-eddy simulation of flows over random urban-like obstacles. Boundary-Layer Meteorol 129:1–23